# PREDICTION OF GLAUCOMATOUS VISUAL FIELD DEFECTS BY REFERENCE PLANE INDEPENDENT THREE-DIMENSIONAL OPTIC NERVE HEAD PARAMETERS

REINHARD O.W. BURK[1], HERBERT NOACK[2], KLAUS ROHRSCHNEIDER[1] and HANS E. VÖLCKER[1]

*[1]Department of Ophthalmology and [2]Institute of Medical Biometry and Medical Informatics, University of Heidelberg, Heidelberg, Germany*

## Abstract

*Purpose:* To evaluate which reference plane-independent topometric optic disc parameters predict glaucomatous visual field defects (GVFD), irrespective of the appearance of the clinical optic nerve head.
*Patients and methods:* Laser scanning tomography was used to analyze the topography of 136 optic discs, preclassified according to computed static white-on-white perimetry into a control group (C, $n$=78) with normal visual fields and a glaucoma group (G, $n$=58) with glaucomatous visual field defects (GVFD). A discriminant analysis, based upon 20 optic cup level reference plane-independent topometric variables, was used to evaluate the maximum classification rate with respect to perimetry. The three best separating variables which predict the presence of GVFD were identified by a stepwise discriminant analysis.
*Results:* The maximum classification rate by a linear combination of 20 topometric variables resulted in a whole non-error rate of 82.4%; 112 of 136 visual field results were predicted correctly by optic disc topography (sensitivity 0.759, specificity 0.872). A robust L1 discriminant analysis of three of these topometric parameters predicted GVFD in 110 of 136 eyes at a whole non-error rate of 80.9% (sensitivity 0.741; specificity 0.859). The following parameters were selected: *1.* The difference between the contour line mean height (CLM difference) in the temporal inferior octant and the temporal quadrant (TQ) of the optic disc (130±80 µm C; 40±110 µm G; $p$<0.0001). *2.* The CLM difference between the temporal superior optic disc octant (TSO) and TQ (180±110 µm C; 80±110 µm G; $p$<0.0001). *3.* The 'optic disc cup-steepness' (third moment of frequency distribution of optic cup depth readings) in the TSO of the optic disc (-0.02±0.13 C; 0.11±0.14 G; $p$<0.0001).
*Discussion:* The results of this cross-sectional study indicate that static perimetry and quantitative three-dimensional optic disc analysis are supplementary tools in the assessment of structural and functional damage in primary open-angle glaucoma at a given stage of the disease. An objective optic disc classification, indicating the risk of existing functional damage as documented in w/w perimetry, may be based upon combinations of reference level independent three-dimensional topometric parameters.

*Address for correspondence:* Professor Reinhard O.W. Burk, Department of Ophthalmology, University of Heidelberg, Im Neuenheimer Feld 400, D-69120 Heidelberg, Germany

*Perimetry Update 1998/1999, pp. 463–474*
*Proceedings of the XIIIth International Perimetric Society Meeting,*
*Gardone Riviera (BS), Italy, September 6–9, 1998*
*edited by M. Wall and J.M. Wild*

## Introduction

The clinical evaluation of glaucoma patients includes optic disc assessment, perimetry and tonometry[1]. There is some evidence that glaucomatous changes in the optic disc and retinal nerve fiber layer (RNFL) may precede the detection of abnormal visual fields, as detected by light discrimination threshold perimetry[2-5]. New imaging techniques are evolving to assess the state of the optic nerve head and RNFL quantitatively. Laser scanning tomography is an accurate and reproducible method that allows for three-dimensional optic disc analysis[7-25]. In this cross-sectional study, we address the question of whether the presence of functional damage from primary open-angle glaucoma (POAG), as documented by white-on-white perimetry, can be predicted by topometric parameters which describe the optic nerve head topography, independent of a clinical prejudgment of whether or not the optic disc shows structural glaucomatous alterations.

## Patients and methods

One hundred and thirty-six reliable and reproducible visual fields (Octopus white-on-white perimetry 6° grid) of patients suffering from POAG, glaucoma suspects, ocular hypertensives, and healthy volunteers, were classified as either glaucomatous (G, *n*=58) or controls (C, *n*=78). All subjects with pathological visual fields were experienced in automated static perimetry. Visual fields were classified as group C when perimetry showed no absolute or relative scotoma at any point outside the blind spot area, compared to age-matched controls[26]. The mean age in group C was 43.2 ± 16.2 years (14-77, median 48.5). The mean refractive error was +0.01 ± 3.9 (-6.75 to +5.0) diopters. The mean threshold sensitivity in group C was 27.9 ± 1.7dB (minimum, 23.4db; maximum 33.9dB).

Classification into group G required at least a cluster of three points with a relative scotoma loss of −5dB or more outside the blind spot area. In cases of doubt, reasons for visual field defects other than glaucoma were ruled out by CT scans of the brain and orbit, Doppler sonography of the carotid artery, and sonography of the optic nerve head. The mean age in group G was 57.7 ± 12.9 years (16-82, median 56.5). The mean refractive error was +0.03 ± 1.4 (-4.0 to +3.5) diopters. The mean threshold sensitivity in group G was 15.8 ± 7.2dB (minimum, 0.5dB; maximum, 27.0dB).

All subjects (group C and G) had a complete ophthalmological examination, including refraction, slit-lamp biomicroscopy, gonioscopy, and fundus three-mirror contact lens examination after pupil dilation.

The optic discs were analyzed by laser scanning tomography (10° image size) after the procedure had been fully explained and informed consent had been obtained. The physical principle of this imaging technique has been described in detail previously[6,16,27]. The clinical appearance of the optic discs in both groups was not considered for classification.

### *Data analysis*

The optic disc border was defined interactively by one of the authors (RB) by drawing a contour line along the disc border on the monitor display of the laser scanning tomograph. In a 10° image, the contour line itself consists of approximately 300-400 pixels (picture elements), depending on the size of the optic disc. Based on the height values of the three-

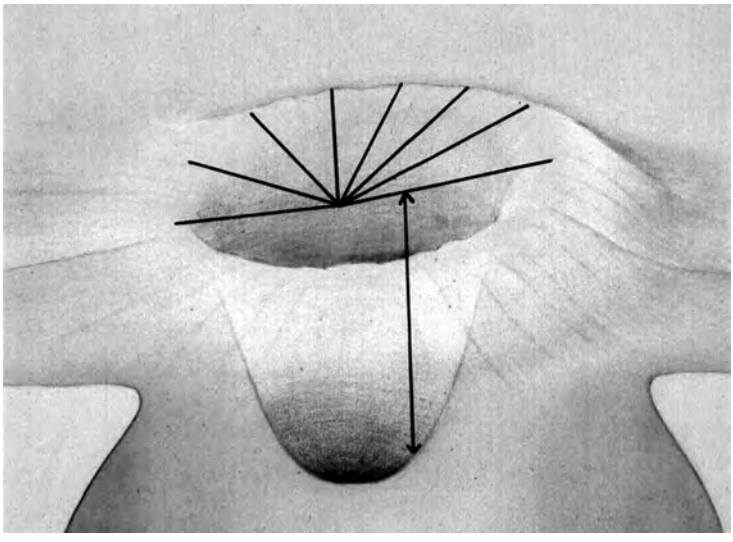

*Fig. 1.* Schematic representation of the curved surface reference plane.

dimensionally defined contour line pixels, a height modulated surface (curved surface) was calculated as a reference plane, which served as an anterior limitation of the optic disc surface towards the vitreous. Because of the ongoing search for an optimal optic disc cup reference level, we based the topographic evaluation for this study on the curved surface alone, without adding a fixed or flexible offset reference level[28]. The curved surface was characterized by the following points (Fig. 1):

1. the height localization at the center point of the surface was the mean height value of the vessel-height corrected optic disc border contour line;
2. the periphery of the surface was fitted onto the contour line at each contour line pixel; and
3. the height variation along each line from the center of the surface to the contour line was linear.

*Topometric parameters*

We defined the following parameters (Table 1) for the three-dimensional analysis of the optic disc surface structure in relation to the optic disc border contour line and the curved surface. These were evaluated in the total optic disc circumference (total, 0° to 360°), the temporal quadrant (TQ) (-45° to +45°), the temporal superior octant (TSO) (+45° to +90°), and the temporal inferior octant (TIO) (-90° to -45°) (Fig. 2). Zero degrees corresponded to the temporal horizontal optic disc limitation.

*Statistical analysis*

*Description of the 23 stereometric variables (topographic parameters)*

We used the Kolmogoroff D-statistic to evaluate whether the 23 variables in the 136 discs were a random sample from a normal distribution ($p<0.05$, Table 2)[29].

*Table 1.* List of the 23 evaluated optic cup level reference plane-independent stereometric parameters for three-dimensional optic nerve head topometry

| | |
|---|---|
| CLM value:<br>(TQ, TSO, TIO; see legend Fig. 2 for segments) | Mean height value of the contour line in the segment under investigation in relation to the mean height value of the total contour line |
| CLM: level difference:<br>(TSO-TQ,TIO-TQ) | Difference between the CLM values of different segments of the optic disc |
| Optic disc area (total = whole optic disc) | Area within the contour line |
| Effective area (total, TQ, TSO, TIO) | Part of the optic disc area with pixel height values below the curved reference surface |
| Curved surface rim area (total) | Optic disc area minus effective area |
| Area ratio (total) | Ratio of effective area and area |
| Volume (total, TQ, TSO, TIO) | All pixels with height values (z-position) below the curved height-modulated surface and within the contour line |
| Mean excavation depth (total) | Ratio of volume and area |
| Maximum excavation depth (total) | Mean depth value of 5% pixels with the largest depth readings within the contour line. The excavation depth at a certain location is the difference between the depth localization of the corresponding pixel and the depth localization of the height-modulated surface at the same axial position |
| 'Steepness' of the optic disc cup<br>(third moment, cup shape measure CSM)<br>(total, TQ, TSO, TIO) | This cup shape parameter is obtained by calculating the third moment of the frequency distribution of depth values below the curved surface, normalized to the half maximum depth[6,7,27]. This shape parameter may have values between +1 and -1. A third moment value of zero indicates symmetric Distribution of excavation depth readings |
| Depth area ratio DAR (total) | ratio of mean depth and mean disc radius |

CLM: contour line modulation

*Significance of parameter mean value differences in the control and glaucoma groups*

The differences in the topometric parameter mean values between optic discs in the visual fields of groups G and C were analyzed using Student's *t* test and the Wilcoxon test. The differences were considered to be significant at $p<0.01$ (Table 3).

*Reclassification into groups based on topographic parameters by discriminant analysis and stepwise discriminant analysis*

Discriminant analysis is a statistical technique in which linear combinations of variables are used to distinguish between the groups under investigation (C versus G). The parameter values were analyzed using the SPSS-X discriminant analysis. All parameters were evaluated to determine the maximum possible classification rate (whole non-error rate), excluding three variables with deterministic linear dependencies to the remaining variables (optic disc area: sum of optic cup area and neuroretinal rim area; CLM-TSO: sum of superior CLM level difference and CLM-TQ; CLM-TIO: sum of inferior CLM level difference and CLM-TQ).

A stepwise discriminant analysis using a cross-validation approach (sample split into a learning sample and a test sample) was then applied in order to find a conservative model

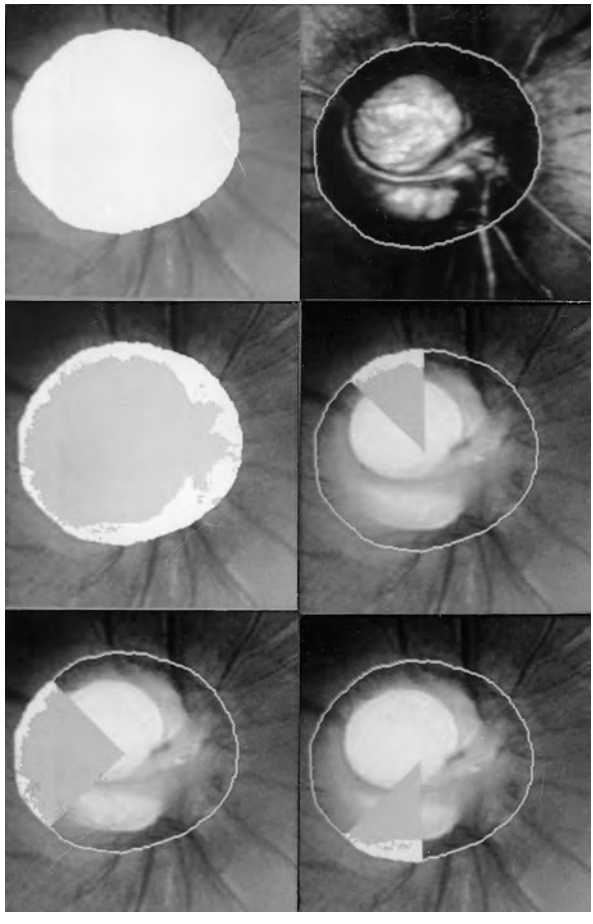

*Fig. 2.* Topometric optic nerve head evaluation within temporal optic disc segments. *Top:* contour line on reflectivity image (right), topographic image with optic disc area (left). *Middle:* curved surface reference plane area (bright) and darkened excavation area (total; left), temporal superior octant (TSO; right). *Bottom:* temporal quadrant (TQ; left) and temporal superior octant (TSO; right).

(only a few variables) to differentiate between optic discs with glaucomatous visual field defects and control group optic discs with normal visual fields[30]. This approach determines which three parameters were the best for dividing optic discs topometrically, according to the perimetric preclassification, into groups G and C. Prior probabilities for the entire sample ($n$=136) were: G: 42.65%; C: 57.35%. To evaluate the effect of changing prior probabilities (priors) on sensitivity and specificity, the lower limit for the whole non-error rate was set at 70%. The receiver operating characteristic (ROC) curve of the resulting canonical discriminant function for the whole sample is presented in Figure 3. Additionally, the three parameters selected were used in a robust L1-discriminant analysis[31].

*Table 2.* Descriptive statistics (mean value ± SD) and Kolmogoroff D-statistic (D) of the 23 variables in 136 discs

| *Parameter* | *Mean ± SD* | *D* | *p (D)* | *Minimum reading* | *Q1* | *Q2* | *Q3* | *Maximum reading* |
|---|---|---|---|---|---|---|---|---|
| Area of optic disc | 2.076 ± 0.504 | 0.064 | n.s. | 0.089 | 1.693 | 2.041 | 2.353 | 3.661 |
| Excavation area (effective area) | 1.384±0.547 | 0.078 | 0.05 | 0.251 | 0.923 | 1.429 | 1.762 | 2.762 |
| Excavation area (TQ) | 0.422±0.139 | 0.059 | n.s. | 0.128 | 0.313 | 0.424 | 0.505 | 0.902 |
| Excavation area (TSO) | 0.196±0.072 | 0.071 | n.s. | 0.006 | 0.145 | 0.207 | 0.246 | 0.358 |
| Excavation area (TIO) | 0.199±0.084 | 0.077 | 0.05 | 0.020 | 0.137 | 0.204 | 0.254 | 0.445 |
| Curved surface rim area | 0.692±0.342 | 0.074 | n.s. | 0.143 | 0.445 | 0.644 | 0.876 | 1.943 |
| Area ratio | 0.653±0.177 | 0.091 | 0.01 | 0.148 | 0.527 | 0.683 | 0.796 | 0.919 |
| Excavation volume | 0.449±0.318 | 0.131 | 0.01 | 0.009 | 0.197 | 0.389 | 0.641 | 1.432 |
| Excavation volume (TQ) | 0.130±0.081 | 0.105 | 0.01 | 0.005 | 0.063 | 0.118 | 0.184 | 0.410 |
| Excavation volume (TSO) | 0.073±0.047 | 0.088 | 0.05 | 0.0 | 0.040 | 0.066 | 0.106 | 0.222 |
| Excavation volume (TIO) | 0.065±0.048 | 0.089 | 0.01 | 0.001 | 0.026 | 0.060 | 0.093 | 0.218 |
| Maximum excavation depth | 0.639±0.228 | 0.055 | n.s. | 0.109 | 0.505 | 0.623 | 0.805 | 1.261 |
| Mean excavation depth | 0.293±0.145 | 0.077 | 0.05 | 0.035 | 0.192 | 0.271 | 0.376 | 0.878 |
| Depth area ratio (DAR) | 0.256±0.172 | 0.082 | 0.05 | 0.007 | 0.135 | 0.228 | 0.341 | 1.073 |
| Third moment | 0.074±0.115 | 0.049 | n.s. | -0.349 | -0.167 | -0.077 | 0.008 | 0.411 |
| Third moment (TQ) | 0.009±0.119 | 0.051 | n.s. | -0.277 | -0.098 | -0.012 | 0.061 | 0.458 |
| Third moment (TSO) | 0.035±0.145 | 0.068 | n.s. | -0.365 | -0.071 | 0.045 | 0.126 | 0.479 |
| Third moment (TIO) | 0.012±0.155 | 0.035 | n.s. | -0.327 | -0.099 | 0.013 | 0.122 | 0.654 |
| CLM (TQ) | -0.117±0.100 | 0.049 | n.s. | -0.392 | -0.195 | -0.110 | -0.043 | 0.156 |
| CLM (TSO) | 0.022±0.086 | 0.084 | 0.05 | -0.378 | -0.023 | 0.030 | 0.072 | 0.266 |
| CLM (TIO) | -0.023±0.090 | 0.084 | 0.05 | -0.332 | -0.079 | -0.013 | 0.035 | 0.359 |
| Level difference (TSO-TQ) | 0.139±0.122 | 0.064 | n.s. | -0.254 | 0.066 | 0.146 | 0.207 | 0.537 |
| Level difference (TIO-TQ) | 0.094±0.103 | 0.057 | n.s. | -0.366 | 0.032 | 0.092 | 0.160 | 0.350 |

Q1: 25% percentile; Q2: 50% percentile (median); Q3: 75% percentile; area values are given in $mm^2$, volume readings in $mm^3$, depth and CLM values in mm. All parameter values are corrected for refractive error and corneal curvature

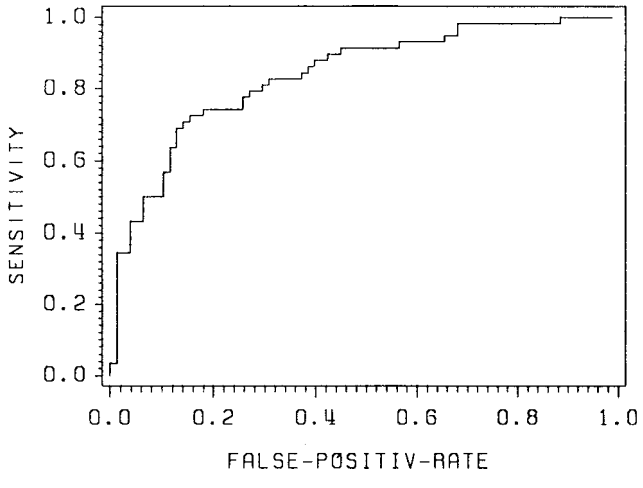


*Fig. 3.* The receiver operating characteristic (ROC) curve for the canonical discriminant function DISC B.

*Table 3.* Parameter mean values and standard deviation

| *Parameter* | *Glaucoma* | *Control* | *Student's t* $p<$ | *Wilcoxon* $p<$ |
|---|---|---|---|---|
| Area (mm²) | 2.12±0.43 | 2.04±0.55 | n.s. | n.s. |
| Effective area (mm²) | 1.58±0.42 | 1.25±0.59 | 0.001 | 0.001 |
| Effective area TQ (mm²) | 0.44±0.12 | 0.41±0.15 | n.s. | n.s. |
| Effective area TSO (mm²) | 0.22±0.06 | 0.18±0.07 | 0.001 | 0.0001 |
| Effective area TIO (mm²) | 0.23±0.06 | 0.18±0.09 | 0.001 | 0.0001 |
| Curved surface rim area | 0.55±0.37 | 0.80±0.29 | 0.001 | 0.0001 |
| Area ratio | 0.75±0.15 | 0.59±0.17 | 0.001 | 0.0001 |
| Cup volume ($mm^3$) | 0.55±0.33 | 0.37±0.29 | 0.001 | 0.001 |
| Cup volume TQ ($mm^3$) | 0.15±0.09 | 0.11±0.07 | 0.01 | n.s. |
| Cup volume TSO ($mm^3$) | 0.09±0.05 | 0.06±0.04 | 0.001 | 0.0001 |
| Cup volume TIO ($mm^3$) | 0.08±0.05 | 0.05±0.04 | 0.001 | 0.001 |
| Depth maximum (mm) | 0.67±0.24 | 0.61±0.22 | n.s. | n.s. |
| Mean depth (mm) | 0.34±0.17 | 0.26±0.12 | 0.01 | 0.01 |
| Depth area ratio | 0.33±0.21 | 0.20±0.11 | 0.001 | 0.0001 |
| Third moment | -0.02±0.11 | -0.11±0.10 | 0.001 | 0.0001 |
| Third moment TQ | 0.05±0.13 | -0.05±0.09 | 0.001 | 0.0001 |
| Third moment TSO | 0.11±0.14 | -0.02±0.13 | 0.001 | 0.0001 |
| Third moment TIO | 0.07±0.16 | -0.03±0.13 | 0.001 | 0.0001 |
| CLM (TQ) (mm) | -0.07±0.10 | -0.15±0.09 | 0.001 | 0.0001 |
| CLM (TSO (mm)) | 0.01±0.11 | 0.03±0.07 | n.s. | n.s. |
| CLM (TIO) (mm) | -0.03±0.11 | -0.02±0.08 | n.s. | n.s. |
| Level difference TSO-TQ (mm) | 0.08±0.11 | 0.18±0.11 | 0.001 | 0.0001 |
| Level difference TIO-TQ (mm) | 0.04±0.11 | 0.13±0.08 | 0.001 | 0.0001 |

Mean value, standard deviation (SD), and *p* values of Student's *t* test and the Wilcoxon test for the topographic parameters in the glaucoma and control groups are listed

## Results

### *Descriptive statistics and Kolmogoroff D-statistic of 23 stereometric parameters in 136 optic discs*

Each optic disc was characterized by 23 variables. Table 2 lists the mean parameter value (mean), standard deviation (SD), minimum and maximum parameter value, as well as the 25% (Q1), 50% (Q2, median) and 75% (Q3) percentile and the Kolmogoroff D-statistic (D) of each single variable in all 136 discs. The data were considered to represent a random sample from a normal distribution in 12 variables ($p>0.05$); in 11 variables we had to reject this assumption ($p<0.05$).

### *Differences between parameter mean values in groups G and C*

Table 3 lists the mean value, SD, *p* values of Student's *t* test and the Wilcoxon test. In 18 of 23 topographic parameter mean values, significant differences ($p<0.01$) existed between optic discs with normal visual fields (C) and optic discs with GVFD (G). In discs with glaucomatous field defects, the cup area for the whole optic disc, temporal superior and temporal inferior optic disc octants, and area ratio (cup/disc area), were greater compared to optic discs with normal fields. The neuroretinal rim area (optic disc area minus cup area)

was smaller and the cup volume and the values for the cup shape measurement were larger in the GVFD group in all optic disc segments evaluated. The mean excavation depth and depth area ratio (DAR) were also greater. Differences between the mean height levels of the contour line between different optic disc segments were smaller in optic nerve heads with glaucomatous visual field defects compared to group C.

In five of the 23 optic cup level independent parameter values, no significant differences existed between groups G and C. These five parameters were optic disc area, cup area in the temporal horizontal quadrant, maximum excavation depth, and mean height positions of the contour line in the temporal superior and temporal inferior octants compared to the total contour line.

*Discriminant analysis: maximum classification rate*

A linear combination of 20 variables classified 112 of the 136 discs (whole non-error rate 82.4%; sensitivity 0.759, specificity 0.872) according to the clinical preclassification based on the presence or absence of visual field defects. All topometric parameters were included in the procedure, except variables with deterministic linear dependencies (area, CLM-TSO, CLM-TIO).

*Stepwise discriminant analysis: cross-validation approach*

To find and evaluate the most selective variables in the stepwise discriminant analysis, the sample of 136 discs was randomly divided (uniform random distribution) into a learning and a test sample: the model for the learning sample was validated in the test sample.
*Test sample:* 70 optic discs (41 control group visual fields, 29 glaucoma visual fields, prior probability G = 41.43%).
*Learning sample:* 66 optic discs (37 control group visual fields, 29 glaucoma visual fields, prior probability G = 43.94%).

*Screening of predictors in the learning sample*

As screening predictors for the learning sample, we selected all variables with a univariate discrimination between the two groups (Student's *t* test and Wilcoxon test, Table 3), excluding remaining variables with deterministic dependencies (area ratio, mean excavation depth, DAR).

*Step statistics: best parameters*

The SPSS-X discriminant analysis uses the Wilks method, which selects the variable that minimizes the overall Wilks $\lambda$. The following three variables are selected in the step statistics:

1. Third moment in the temporal superior octant (Wilks $\lambda$ =0.778; F to enter = 18.22).
2. CLM level difference between the temporal inferior octant and the temporal horizontal quadrant TIO-TQ (Wilks $\lambda$= 0.695; F to enter = 7.58).
3. CLM level difference between the temporal superior octant and the temporal horizontal quadrant TSO-TQ (Wilks $\lambda$ = 0.651; F to enter = 4.19)

Summary statistics for the discriminant function:

Wilks $\lambda = 0.651$ ($\chi^2 = 26.82$ df = 3 $p<0.0001$). Canonical correlation: 0.591.

*Canonical discriminant function*

Based on the topographic parameter values from the learning sample, the following canonical discriminant function (DISC) results were obtained:

DISC A (learning sample)
= 3.765 (CLM TSO-TQ) + 4.970 (CLM TIO-TQ) - 3.975 (third moment TSO) - 0.724
(if DISC> = 0 classifies as control, if DISC < 0 classifies as glaucoma)

When we used all the information from the 136 discs to discover the best discriminant function between the control group and the glaucoma group with the three selected variables, the coefficients were slightly different:

DISC B (whole sample)
= 4.197 (CLM TSO-TQ) + 5.642 (CLM TIO-TQ) - 3.885 (third moment TSO) - 0.974
(if DISC > = 0 classifies as control, if DISC < 0 classifies as glaucoma)

*Error rates*
When we used the canonical discriminant function from the learning sample (DISC A) to classify the learning and test samples, the whole non-error rate for the learning sample was 80.3% (sensitivity 0.793, specificity 0.813) and for the test sample 78.6% (sensitivity 0.621, specificity 0.902).

When we used the discriminant function fitted with all the information from 136 eyes (DISC B) to classify the whole sample, no better non-error rate (77.2%) was found, but a higher sensitivity compared to the test sample results was present. The outcome of perimetry could be predicted in 105 of 136 optic discs (77.2%): 43 of 58 (74.1%) optic discs in group G and 62 of 78 eyes (79.5%) in group C could be classified in this conservative model. Changing priors into $p$ (C) = 0.30 and $p$ (G) = 0.70 led to a sensitivity of 0.914 and specificity being reduced to 0.564 (whole non-error rate 71.3%). The ROC curve of DISC B is shown in Figure 3. In a robust L1-discriminant analysis, the whole non-error classification rate using the three best separating topometric variables increased to 80.9%, due to a higher specificity (sensitivity 0.741, specificity 0.859).

## Discussion

In this study, we evaluated three-dimensional optic disc surface topography in optic nerve heads with and without visual field defects from POAG using optic cup level independent stereometric variables. It is important to emphasize that the classification into a glaucoma group and control group was based on the results of perimetry alone. The appearance of the optic disc was not considered, because it was our aim to evaluate optic nerve head topography as objectively as possible, without a bias from preselection based upon clinical definitions. Perimetry as the only clinical discriminant factor was chosen in order to analyze whether three-dimensional topometric parameters exist that might be useful for indicating the presence of visual field defects, independent of any clinical knowledge-based prejudgment according to optic nerve head morphology. Because of this strict preclassification, the

control group, by definition, did not consist only of 'normal optic discs'; glaucomatous optic discs changes were included and accepted in this group as long as the visual field was perfectly normal, as indicated by white-on-white perimetry.

Eighteen of 23 topographic parameters tested showed significantly ($p<0.01$) different mean values in association with glaucomatous visual field defects. As would be expected from clinical practice, the presence of visual field defects as detected by 6° white-on-white perimetry was associated with greater values for stereometric parameters which indicate tissue loss such as 'depth area ratio', area ratio (excavation area to disc area), total and segmental excavation areas, excavation volumes and the shape parameter 'cup steepness' (third moment of the frequency distribution of excavation depth readings). In the group of optic discs with GVFD, the contour line modulation differences between the temporal superior and inferior octants and the temporal quadrant of the optic disc were reduced, thus indicating an overall flattening of the retinal surface contour along the optic disc border in glaucoma, in contrast to optic nerve heads with normal visual fields[32].

We found no significant differences between the groups for optic disc area, maximum excavation depth, relative position of the contour line in the temporal superior and temporal inferior octants compared to the total contour line and excavation area in the temporal quadrant. This latter finding corresponded to the well-known phenomenon that glaucomatous structural alterations are more likely to occur in the inferior and superior temporal octants of the optic nerve head. This confirms the theory that progressive glaucomatous cupping may be more pronounced in a vertical direction than a horizontal expansion[33-36].

Despite the significant difference in many parameter mean values, no single topometric variable was found to reliably predict the functional state of an optic disc because of the enormous interindividual variability of optic nerve head topography, as indicated by the standard deviations of the variables under evaluation.

Using only three of the parameters, 110 of 136 eyes (80.9%) could be classified correctly with a sensitivity of 0.741 at a specificity of 0.859. It is important to note that, by not using an optic cup level reference plane which was introduced by us as the standard reference plane for the Heidelberg Retina Tomograph[28], the three selected parameters relied on depth information, but were independent of the size of the optic disc. Parameters which describe optic disc area values are not included in the stepwise statistical analysis. In similar approaches, where our standard reference plane was used, sensitivity and specificity were reported as being 87% at 84% and 78% at 88%, respectively[37,38]. In these studies, the third moment, as a reference plane independent shape parameter, was also selected among the important variables. The slightly higher figures with respect to the whole non-error classification rates obtained with the use of the standard reference plane are encouraging, indicating that this reference level determination is clinically meaningful in independent observations. However, our aim was to evaluate surface topography variables which may separate preclassified optic nerve heads, irrespective of their clinical appearance. In this respect, the differences in relative height variations of the retinal surface along the border of the optic disc are important. In POAG, a remarkable flattening of the optic disc contour line can be observed using scanning laser tomography[32]. An analogous phenomenon has been found for the peripapillary nerve fiber layer contour using computerized analysis of simultaneous stereo video recordings and stereophotogrammetry[39,40].

Laser scanning tomography is a non-invasive diagnostic tool that provides objective information about the optic disc topography to the observer. Using tonometry to assess major risk factors for POAG, and perimetry to measure the functional state of the eye, the introduction of optic disc topometry to evaluate the site of glaucomatous tissue damage

will become the third cornerstone in the diagnosis and follow-up of patients suffering from POAG, or of glaucoma suspects. Further studies on larger samples of optic nerve heads are needed to establish the usefulness of this discriminant function, together with other optic cup level reference plane-based equations, in the prediction of the onset of glaucomatous visual field defects by stereometric parameters.

## Acknowledgment

This study was supported by a grant from the Deutsche Forschungsgemeinschaft DFG Vo 437/1-2.

## References

1. The American Academy of Ophthalmology Quality of Care Committee Glaucoma Panel: Primary open-angle glaucoma. Preferred Practice Pattern 1-31, 1989
2. Quigley HA, Dunkelberger GR Green WR: Retinal ganglion cell atrophy correlated with automated perimetry in human eyes with glaucoma. Am J Ophthalmol 107:453-464, 1989
3. Tuulonen A, Airaksinen PJ: Initial glaucomatous optic disc and retinal nerve fiber layer abnormalities and their progression. Am J Ophthalmol 111:485-490, 1991
4. Sommer A, Katz J, Quigley HA et al: Clinically detectable nerve fiber layer atrophy precedes the onset of glaucomatous visual field loss. Arch Ophthalmol 109:77-83, 1991
5. Quigley HA, Katz J, Derick RJ, Gilbert D, Sommer A: An evaluation of optic disc and nerve fiber layer examinations in monitoring progression of early glaucoma damage. Ophthalmology 99:19-28, 1992
6. Zinser G, Harbarth U, Schröder H: Formation and analysis of three-dimensional data with the laser tomographic scanner LTS. In: Nasemann JE, Burk ROW (eds) Laser Scanning Ophthalmoscopy and Tomography, Ch 24, pp 243-252. München: Quintessenz 1990
7. Burk ROW, Rohrschneider K, Noack H, Völcker HE: Volumetrische Papillenanalyse mit Hilfe der Laser-Scanning-Tomographie. Klin Mbl Augenheilk 198:522-529, 1991
8. Burk ROW, Rohrschneider K, Noack H, Völcker HE: Are large optic nerve heads susceptible to glaucomatous damage at normal intraocular pressure? Graefe's Arch Clin Exp Ophthalmol 230:552-560, 1992
9. Burk ROW, Rohrschneider K, Völcker HE, Takamoto T, Schwartz B: Laser scanning tomography and stereophotogrammetry in three-dimensional optic disc analysis. Graefe's Arch Clin Exp Ophthalmol 231:193-198, 1993
10. Weinreb RN, Lusky M, Bartsch DU, Morsman D: Effect of repetitive imaging on topographic measurements of the optic nerve head. Arch Ophthalmol 111:636-638, 1993
11. Burk ROW, König J, Rohrschneider K, Noack H, Völcker HE: [3-dimensional topography of the optic papilla with laser scanning tomography: clinical correlation of cluster analysis] Dreidimensionale Papillentopographie mittels Laser Scanning Tomographie. Klinisches Korrelat einer Cluster-Analyse. Klin Mbl Augenheilk 204:504-512, 1994
12. Rohrschneider K, Burk ROW, Kruse FE, Völcker HE: Reproducibility of the optic disc nerve head topography with a new laser tomographic scanning device. Ophthalmology 101:1044-1049, 1994
13. Chauhan BC, LeBlanc RP, McCormick TA, Rogers JB: Test-retest variability of topographic measurements with confocal scanning laser tomography in patients with glaucoma and control subjects. Am J Ophthalmol 118:9-15, 1994
14. Janknecht P, Funk J: Optic nerve head analyzer and Heidelberg Retina Tomograph: accuracy of topographic measurements in a model eye and in volunteers. Br J Ophthalmol 78:760-768, 1994
15. Bartz-Schmidt KU, Weber J, Heimann K: Validity of two-dimensional data obtained with the Heidelberg Retina Tomograph as verified by direct measurements in normal optic nerve heads. German J Ophthalmol 3:400-405, 1994
16. Burk ROW, Völcker HE: Scanning laser ophthalmoscopy and tomography. In: Jay B, Kirkness CM (eds) Recent Advances in Ophthalmology, Vol 9, pp 225-243. Edinburgh: Churchill Livingstone 1995
17. Chauhan BC, McCormick TA: Effect of the cardiac cycle on topographic measurements using confocal scanning laser tomography. Graefe's Arch Clin Exp Ophthalmol 233:568-572, 1995

18. Bartz-Schmidt KU, Sengersdorf A, Esser P, Walter P, Hilgers RD, Krieglstein GK: The cumulative normalised rim/disc area ratio curve. Graefe's Arch Clin Exp Ophthalmol 234:227-231, 1996
19. Kono Y, Qi-min C, Tomita G, Yamamoto T, Kitazawa Y: High-pass resolution perimetry and a Humphrey field analyzer as indicators of glaucomatous optic disc abnormalities. Ophthalmology 104:1496-1502, 1997
20. Anton A, Yamagishi N, Zangwill L, Sample PA, Weinreb RN: Mapping structural to functional damage in glaucoma with standard automated perimetry and confocal scanning laser ophthalmoscopy. Am J Ophthalmol 125:436-446, 1998
21. Broadway DC, Drance SM, Parfitt CM, Mikelberg FS: The ability of scanning laser ophthalmoscopy to identify various glaucomatous optic disc appearances. Am J Ophthalmol 125:593-604, 1998
22. Burk ROW, Tuulonen A, Airaksinen PJ: Laser scanning tomography of localised nerve fibre layer defects. Br J Ophthalmol 82:1112-1117, 1998
23. Caprioli J, Park HJ, Ugurlu S, Hoffman D: Slope of the peripapillary nerve fibre layer surface in glaucoma. Invest Ophthalmol Vis Sci 39:2321-2328, 1998
24. Teesalu P, Vihanninjoki K, Airaksinen PJ, Tuulonen A: Hemifield association between blue-on-yellow visual field and optic nerve head topographic measurements. Graefe's Arch Clin Exp Ophthalmol 236:339-345, 1998
25. Wollstein G, Garway-Heath DF, Hitchings RA: Identification of early glaucoma cases with the scanning laser ophthalmoscope. Ophthalmology 105:1557-1563, 1998
26. Heijl A, Lindgren G, Olsson J: Normal variability of static perimetric threshold values across the central visual field. Arch Ophthalmol 105:1544-1549, 1987
27. Burk ROW, Rohrschneider K, Völcker HE, Zinser G: Analysis of three-dimensional optic disc topography by laser scanning tomography. In: Nasemann JE, Burk ROW (eds) Laser Scanning Ophthalmoscopy and Tomography, Ch 15, pp 161-176. München: Quintessenz 1990
28. Burk ROW, Vihanninjoki K, Bartke Th, Tuulonen A, Airaksinen PJ, Völcker HE, König JM: Development of the standard reference plane for the Heidelberg Retina Tomograph HRT. Graefe's Arch Clin Exp Ophthalmol 1999 (in press)
29. Sachs L. Applied Statistics, Ch 4.4. New York, NY: Springer 1984
30. Armitage P, Berry G: Statistical Methods in Medical Research: Multivariate Methods, 2nd Edn, Ch 10.5. Oxford: Blackwell 1987
31. Krusinska E: $L_p$-logistic discrimination. Appl Math Lett 1:357-360, 1988
32. Burk ROW, Rohrschneider K, Völcker HE: Posterior segment laser scanning tomography: contourline modulation in optic disc analysis. Proc SPIE 1357:228-235, 1990
33. Armaly MF: Optic cup in normal and glaucomatous eyes. Invest Ophthalmol 9:425-429, 1970
34. Gloster J: Vertical ovalness of glaucomatous cupping. Br J Ophthalmol 59:721-724, 1975
35. Pederson JE, Anderson DR: The mode of progressive disc cupping in ocular hypertension and glaucoma. Arch Ophthalmol 98:490-495, 1980
36. Airaksinen PJ, Alanko HI: Effect of retinal nerve fibre loss on the optic nerve head configuration in early glaucoma. Graefe's Arch Clin Exp Ophthalmol 220: 193-196, 1983
37. Mikelberg FS, Parfitt CM, Swindale NV, Graham SL, Drance SM, Gosine R: Ability of the Heidelberg Retina Tomograph to detect early glaucomatous visual field loss. J Glaucoma 4:242-247, 1995
38. Bathija R, Zangwill L, Berry CC, Sample PA, Weinreb RN: Detection of early glaucomatous structural damage with confocal laser scanning tomography. J Glaucoma 7:121-127, 1998
39. Caprioli J, Miller JM. Measurement of relative nerve fibre layer surface height in glaucoma. Ophthalmology 96:633-639, 1989
40. Takamoto T, Schwartz B: Photogrammetric measurement of nerve fiber layer thickness. Ophthalmology 96:1315-1319, 1989